



Investigation and Comparison of In-Flight Particle Velocity During the Plasma-Spray Process as Measured by Laser Doppler Anemometry and DPV-2000

G. Mauer, R. Vaßen, S. Zimmermann, T. Biermordt, M. Heinrich, J.-L. Marques, K. Landes, and J. Schein

(Submitted September 26, 2012; in revised form April 10, 2013)

Plasma spraying has become one of the most important thermal-spray technologies due to low operating costs, high deposition rates, and a high efficiency. It is especially suitable for producing coatings used to improve thermal, corrosion, and wear protection. The quality of coatings produced by thermal-spray processes are determined by particle characteristics, such as in-flight velocity, which can be investigated using various diagnostic systems. Velocity is a particularly relevant parameter for small particles, but it is difficult to measure. Hence, different velocity diagnostics must be validated for small injected particles. We compared the laser Doppler anemometry (LDA) system with the DPV-2000 system and measured the particle velocities of a F4 plasma torch. The results agreed well when the limited detectability of small particles by LDA was taken into account.

Keywords atmospheric plasma spray (APS), optical diagnostics, optical sensors, particle flight, particle temperature, particle trajectories, particle velocity

cathode surrounded concentrically by the plasma gas flow and a one-piece nozzle operating as the anode is shown in Fig. 1 (Ref 4, 5).

1. Introduction

1.1 Thermal Spraying: Plasma-Spraying Process

Thermal spraying is a coating deposition technique. Powder or wire materials are heated to a molten or partially molten state by certain heat sources (such as electric arc, flame, plasma, and laser, etc.). The molten droplets are accelerated to impinge on the substrate at high velocities, solidify, and form the coating. The thermal-spraying method and spray materials primarily determine the coating quality (Ref 1–3). Among current thermal-spraying methods, the plasma-spray process using conventional DC discharge plasma torches is widely used in industry. Different construction principles exist with single or multiple electrodes (cathode, anode) as well as with one-piece or cascaded nozzles. A conventional DC plasma torch with a rod-shaped tungsten

Nomenclature

q	Mie parameter
d_p	Particle diameter
λ_{Laser}	Wavelength of the laser beam
d	Distance between two consecutive maxima and minima
v_x	Velocity component perpendicular to the interference fringes
Θ	Angle between the two incident laser beams
α	Angle between the flow direction and the interference fringes
f	Frequency
\vec{k}_1, \vec{k}_2	Wave vectors
\vec{k}_S	Scattering wave vector
\vec{e}	Unit vector
Δf_D	Doppler shift (frequency)
d_{slit}	Distance of the slits
N	Fringe value
l_x, l_y, l_z	Parameter of the LDA-measurement volume
f_{magn}	Magnification factor
v_p	Particle velocity
T_p	Particle temperature
S_p	Particle shape
n_p	Particle number density
$E(\lambda_i)$	Energy
λ_i	Wavelength
c_2	Constant

G. Mauer, and R. Vaßen, IEK-1, Forschungszentrum Jülich GmbH, 52425 Jülich, Germany; and S. Zimmermann, T. Biermordt, M. Heinrich, J.-L. Marques, K. Landes, and J. Schein, EIT1 IPM (LPT), Universität der Bundeswehr München, 85577 Neubiberg, Germany. Contact e-mails: Stephan.Zimmermann@UniBw.de and G.Mauer@fz-juelich.de.

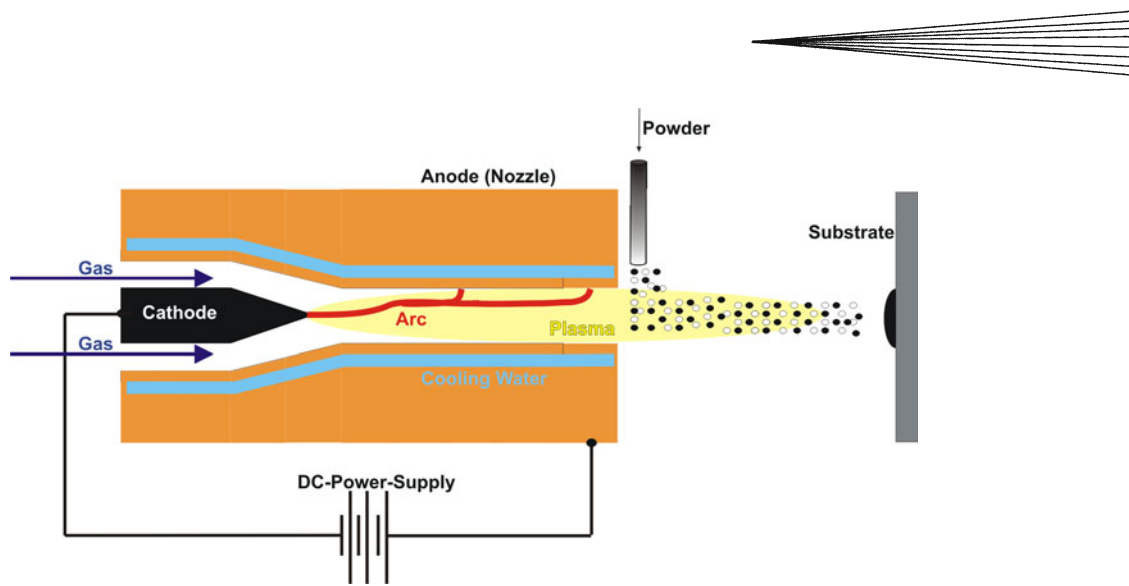


Fig. 1 Plasma-spray process with conventional DC plasma torch (F4-type)

1.2 Particle Diagnostics During the Thermal-Spray Process

High-quality plasma-sprayed coatings require a uniform treatment of the particles injected by the plasma jet. Diagnostic systems (Ref 6, 7) help us to understand the fundamental characteristics and physics of the spray process. These analytic systems focus on one or more significant particle properties (temperature, velocity, number density, etc.). The measurement principles (Ref 6–10) are based on different physical effects, e.g., scattering, radiation, and absorption. Such diagnostic systems provide results helping us improve the process, and they are also used as validation or start data in numerical computer simulations. Thermal-spray diagnostics can be divided into four areas of application (system diagnostics, flame or plasma diagnostics, particle diagnostics, coating diagnostics, and tests). Table 1 provides an overview of typical particle diagnostics (Ref 11–15).

Our main goal was to identify spray parameters (distance, temperature, pressure, etc.) for optimal coating properties, as well as to monitor the process conditions. The kinetic and thermal characteristics of the powder particles determine the quality of the coating. The most important particle properties are (Ref 6, 7, 10) size d_p , shape S_p , number density n_p , velocity \vec{v}_p , and temperature T_p . Many diagnostic systems have been developed to obtain information about these properties and most of them are well suited for online operation.

2. Principles of the Particle Diagnostic Systems

2.1 Laser Doppler Anemometry

Laser Doppler anemometry (LDA) is a flexible and well-established nonintrusive method of investigating the

Table 1 Overview of different particle diagnostics

Particle diagnostic systems	\vec{v}_p	T_p	n_p	d_p	S_p
DPV 2000					
Flux Sentinel					
AccuraSpray					
Spray Watch					
ThermaViz					
PIV (Particle Image Velocimetry)					
LDA (Laser Doppler Anemometry)					
PDA (Phase Doppler Anemometry)					
L2F (Laser Two Focus)					
NIR-Sensor					
PSI (Particle Shape Imaging)					
VisiSizer					

■ direct result ■ calculated result

local velocity components of gases, liquids, and multi-component flow mixtures with the help of tracer particles. In this case, LDA was used to investigate thermal spraying, whereby the particles of the injected spray powder served as tracer particles. This allows the velocity of injected powder particles to be measured. In addition, the velocity of the powder-carrying plasma flow can be determined. However, a lag between the particles and the particle-carrying medium has to be taken into account. Commercial LDA configurations are available from DantecDynamics and TSI (Ref 12–14), and interesting setups and developments (e.g., mobile robust system miniaturization) have been accomplished. LDA is based on the principle of light scattering, whereby particles are illuminated by a laser beam (Fig. 2). It can be described by Mie theory. The light-scattering process is classified according to the Mie parameter q , which describes the

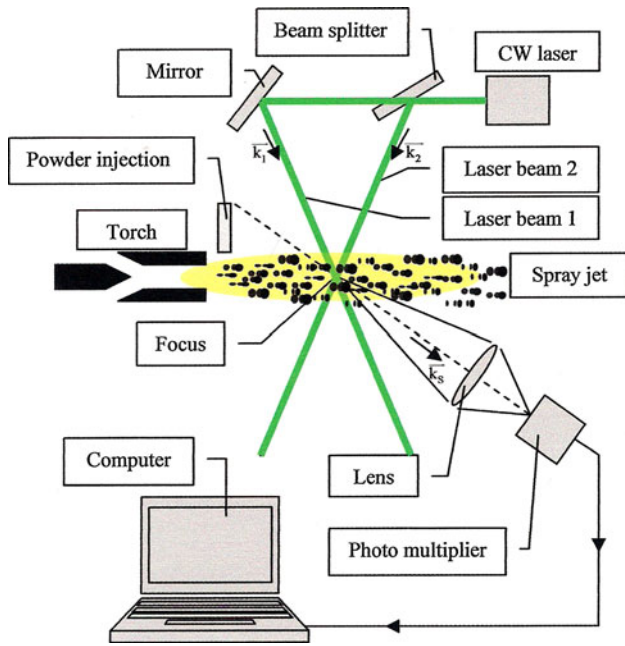


Fig. 2 Experimental setup used for LDA

ratio between size and the incident wavelength and is defined as

$$q = \frac{\pi d_p}{\lambda_{\text{laser}}}, \quad (\text{Eq 1})$$

where d_p is the particle diameter, and λ_{laser} is the wavelength of the laser beam. Scattering is thus divided into $q \ll 1$ Rayleigh scattering, $q \approx 1$, $q > 1$ Mie scattering (the typical range for LDA), and $q \gg 1$ applied for geometrical optics. Figure 3 represents the dependence between maximum, minimum, and the velocity component perpendicular to the interference fringes. The LDA measurement volume in our case is built by the following parameters: MV-measurement volume ($l_x = 0.32 \text{ mm} \times l_y = 21.34 \text{ mm} \times l_z = 0.32 \text{ mm}$ ellipsoid, fringe value $N = 37$), laser beam radius 0.16 mm, focus lens 1000 mm, laser wavelength 532 nm, and LDA 2Θ -angle 1.7188° . The LDA process can be explained in two alternative but equivalent ways (Ref 9, 16–20): as an interference pattern and by means of the Doppler effect. To produce an interference pattern, two laser beams are superposed in the measurement volume to produce a periodic pattern of intensity maxima and minima parallel to the bisecting line of the beams (Fig. 3). The distance d between two consecutive maxima and minima is $d = \frac{\lambda_{\text{laser}}}{2 \sin(\Theta/2)}$, where Θ is the angle between the two incident laser beams. These particles flying through the measurement volume produce a periodic scattering signal (frequency f), when crossing the interference fringes. A photomultiplier records these signal. The velocity component v_x perpendicular to the interference fringes is calculated according to

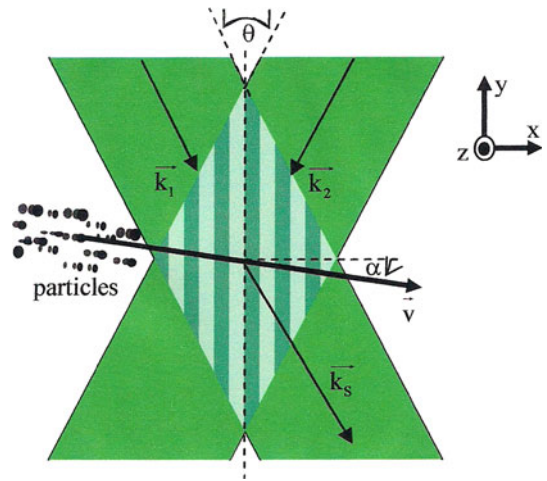


Fig. 3 LDA measurement volume (interference fringe pattern)

$$v_x = df = \frac{\lambda_{\text{laser}} f}{2 \sin(\Theta/2)}. \quad (\text{Eq 2})$$

The intensity of the signal depends on the detection direction and the object size (particle diameter). Assuming spherical particles and using Mie theory (Ref 10, 21), this angular function can be determined. Alternatively, the Doppler shift in the light scattered by the flying particles can be used. The Doppler effect occurs twice, once when the incident laser light (beam 1 with wave vector k_1 and beam 2 with wave vector k_2) of the transmitter system, characterized by the wavelength $\lambda_{\text{laser}} = \frac{2\pi}{k_1} = \frac{2\pi}{k_2}$ and frequency $f_{\text{laser}} = f_1 = f_2$ impinges on the moving target (velocity \vec{v}), and once when the light with frequencies f_{p1} and f_{p2} (subscript p for particle; subscripts 1 and 2 for laser beams 1 and 2) is scattered by the moving particle and received by the detector with frequencies f_{r1} and f_{r2} (subscript r for receiver). The frequency shifts are calculated by

$$\Delta f_{p1} = f_{p1} - f_{\text{laser}} = -\frac{\vec{k}_1 \cdot \vec{v}}{2\pi} \quad (\text{Eq 3})$$

$$\text{and } \Delta f_{p2} = f_{p2} - f_{\text{laser}} = -\frac{\vec{k}_2 \cdot \vec{v}}{2\pi};$$

$$\Delta f_{r1} = f_{r1} - f_{\text{laser}} = -\frac{\vec{k}_1 \cdot \vec{v}}{2\pi} + \frac{\vec{k}_s \cdot \vec{v}}{2\pi} \quad (\text{Eq 4})$$

$$\text{and } \Delta f_{r2} = f_{r2} - f_{\text{laser}} = -\frac{\vec{k}_2 \cdot \vec{v}}{2\pi} + \frac{\vec{k}_s \cdot \vec{v}}{2\pi}.$$

The difference Δf_D between the two frequencies of the light components scattered by the moving particle and recorded by the photo multiplier is

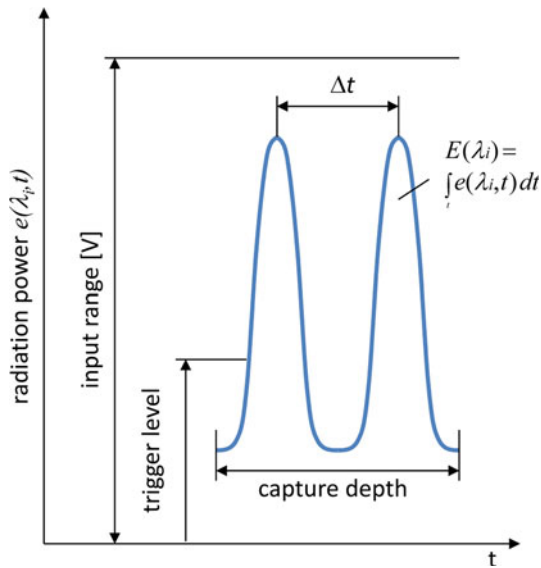
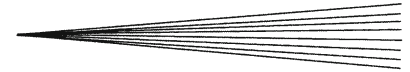


Fig. 4 Basic principles of the particle diagnostic system DPV-2000

$$\Delta f_D = f_{r2} - f_{r1} = \Delta f_{r2} - \Delta f_{r1} = \frac{\vec{k}_1 \cdot \vec{v}}{2\pi} + \frac{\vec{k}_2 \cdot \vec{v}}{2\pi} = \frac{(\vec{k}_1 - \vec{k}_2) \cdot \vec{v}}{2\pi} \quad (\text{Eq 5})$$

Using $|\vec{k}_1 - \vec{k}_2| = 2|\vec{k}| \sin(\frac{\Theta}{2}) = \frac{4\pi}{\lambda_{\text{laser}}} \sin(\frac{\Theta}{2})$, the particle velocity component v_x can be determined:

$$v_x = \frac{\Delta f_D \lambda_{\text{laser}}}{2 \sin(\Theta/2)} \quad (\text{Eq 6})$$

2.2 DPV-2000 Particle Diagnostic System

The DPV-2000 (Ref 11) enables measuring particle velocities, temperatures, and diameters. Figure 4 shows the basic operating principles of the system. The velocity is obtained by determining the time between two signals triggered by a radiating particle passing the two-slit mask of the optoelectronic sensor head. In conjunction with the distance of the slits d_{slit} and the magnification factor of the lens, f_{magn} the particle velocity v_p can be calculated by

$$v_p = \frac{d_{\text{slit}}}{\Delta t} f_{\text{magn}} \quad (\text{Eq 7})$$

The particle temperature T_p is acquired by two-color pyrometry, i.e., by calculating the ratio of the energy $E(\lambda_i)$ radiated at two different wavelengths λ_i assuming that the particles are gray-body emitters with the same emissivity at both color bands by

$$T_p = \frac{c_2 \left(\frac{1}{\lambda_1} - \frac{1}{\lambda_2} \right)}{\ln \left(\frac{E(\lambda_1)}{E(\lambda_2)} \left(\frac{\lambda_1}{\lambda_2} \right)^5 \right)} \quad (\text{Eq 8})$$

where $c_2 = 1.438775 \cdot 10^{-2}$ mK is a constant. The particle diameter d_p is obtained from the radiation energy emitted at one wavelength, assuming that the melted particles are spherical or almost spherical by

$$d_p = \sqrt{\frac{E(\lambda_i)}{f_{\text{diam}}}} \quad (\text{Eq 9})$$

Since it is necessary to know the real emissivity of the particle, usually a powder with known diameter distribution has to be measured in advance to determine the calibration factor f_{diam} . However, since possible changes in emissivity with temperature or molten state could affect the accuracy of particle size measurement for a given calibration, the size distributions of the powders applied in this study were independently measured by laser diffraction, and the DPV was calibrated correspondingly as described later. As the measurement volume is relatively small ($<1 \text{ mm}^3$), the data are collected for individual particles and can subsequently be analyzed statistically. A certain measurement time is necessary to support the mean and standard deviations by sufficient individual particle number of datasets (Ref 22–24).

3. Experimental Setups

3.1 Experimental Environment

Measurements of the in-flight particle velocity of the plasma-sprayed particles were performed at IEK-1, Forschungszentrum Jülich GmbH. Two different diagnostic methods were compared. One of them was LDA, which was set up and operated by IPM at the Universität der Bundeswehr. The other diagnostic system was the DPV-2000 [TECNAR Automation Ltd., St-Bruno, QC, Canada (Ref 11, 23)], which was operated by Forschungszentrum Jülich, IEK-1. The comparative measurements were carried out on a Multicoat™ facility (Sulzer Metco, Wohlen, Switzerland) during atmospheric plasma spraying with a single-cathode F4 gun. The spray parameters are listed in Table 2.

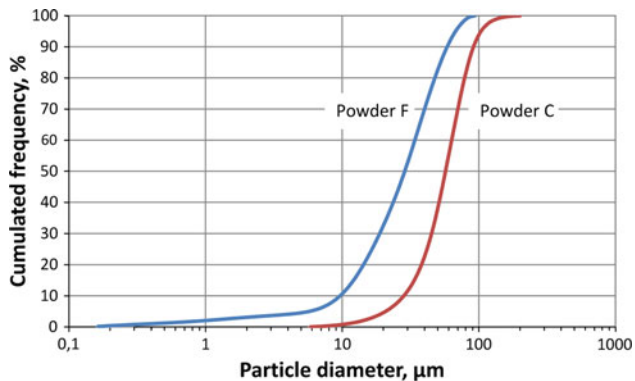
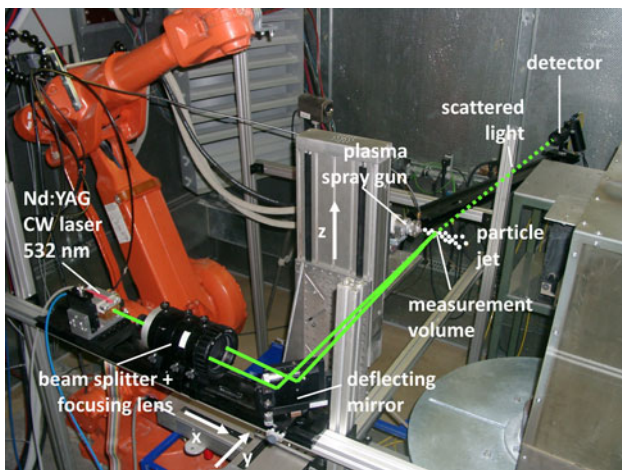
Two 8 wt.% yttria partially stabilized, zirconia-spray-dried powders were used. The finer powder (in the following, designated F) was a Sulzer Metco 204NS-G (−106/+11 μm). The particle diameters determined by laser diffraction were $d_{10} = 8 \text{ μm}$, $d_{50} = 26 \text{ μm}$, and $d_{90} = 51 \text{ μm}$. The coarser powder (in the following, designated C) was a Sulzer Metco 204NS (−125/+11 μm). The particle diameters determined by laser diffraction were $d_{10} = 28 \text{ μm}$, $d_{50} = 57 \text{ μm}$, and $d_{90} = 92 \text{ μm}$. Figure 5 shows the measured particle size distributions. The morphology was spheroidal due to the manufacturer’s proprietary HOSP™ process (Sulzer Metco Europe GmbH, Kelsterbach, Germany).

3.2 Laser Doppler Anemometry

The system was developed by the Universität der Bundeswehr München. The principal setup was built comprising a CW laser (coherent, type Compass 315M, Nd-YAG Laser 100 mW), a photodetector (Dantec Type 57X08PM (500 MHz)), and a computer (ASYST software). The measuring positions within the plasma jet are arranged in a quadratic planar grid perpendicular to the

Table 2 F4 plasma-spray parameters

Current	600 A
Input power	39.2 kW
Plasma gas	40 slpm Ar, 10 slpm H ₂
Carrier gas	3.5 slpm Ar
Powder feed disk	5%
Powder feed rate	8 g/min
Stand-off distance	100 mm

**Fig. 5** Particle size distributions of the applied YSZ powder feedstock determined by laser diffraction method**Fig. 6** Measurement setup for laser Doppler anemometry

gun axis. The center point of the grid is positioned on the gun axis. The gun was moved by an x - y - z positioning unit so that the grid points were subsequently located in the measurement volume (Fig. 6) (Ref 8, 25). The measurement time per grid point was 1 s or less if the maximum number of 1500 detected particles had been reached earlier. In the periphery of the measurement grid, only very few particles were detected. As their characteristics are not representative for the total particle fraction, the results at these points were not considered. At every point of the grid, a complete evaluation was carried out, the results of which can be presented in different ways (his-

togram of velocity distribution, contour plots of number density or velocity) (Ref 8, 25).

3.3 DPV-2000 Particle Diagnostic System

For the DPV-2000 measurements (Ref 11, 22–24), the gun was positioned at a fixed location, and the measurement head was moved in the y - z plane perpendicular to the gun axis at a spray distance of $x = 100$ mm (Fig. 7). The 13×13 point measurement grid was 30×30 mm². The measurement time per grid point was 10 s or less if the maximum number of 1000 detected particles had been reached earlier. In our measurements, we did not find any further statistical improvement of the results if more than 1000 particles were evaluated. The measurement head was adjusted so that the measurement grid was centered at the location of maximum particle flow. Again, the results at grid points in the periphery of the grid were not considered because very few particles were detected there.

4. Measurement Results and Discussion

Initially, two LDA measurements (denoted LDA 1 and LDA 2) were performed with powder F at a spray distance of $x = 100$ mm in the planes perpendicular to the gun axis: LDA 1 on a 11×11 point grid measuring 80×80 mm², and LDA 2 on a 13×13 point grid measuring 60×60 mm². The DPV results were obtained on a 13×13 point grid measuring 30×30 mm² at the same spray distance. Shorter or longer spray distances than this operational stand-off were not investigated.

In order to compare the LDA and the DPV-2000 results, the measurement grids of both methods must be congruent. As they were not located at physically identical positions, the grids were aligned with each other by horizontal and vertical displacement of the DPV grid. Only the qualitative shape of the curves is suitable as a criterion for agreement because the measured results are quantitatively different. The speeds achieved by the DPV-2000 averaged approximately 25% higher than those obtained by LDA. Figure 8 shows the vertical and horizontal developments of the measured particle velocities through the center points of the measurement grids when they were aligned with each other. The two LDA results show good reproducibility. Qualitatively, the LDA and DPV curves are fairly in good agreement. The quantitative differences between the results of the two methods will be discussed in the following.

The two diagnostic methods LDA and DPV-2000 generally have limited capabilities for detecting small particles. According to Mie theory, the intensity of the light scattered by the particles depends among other parameters on the particle size. Thus, the sensitivity of the LDA detector is determined by the smallest measurable particle size. The DPV-2000 measurements are based on the particle thermal radiation. The radiated power is determined by the particle temperature, by its surface area, and by the emissivity of the material. This means

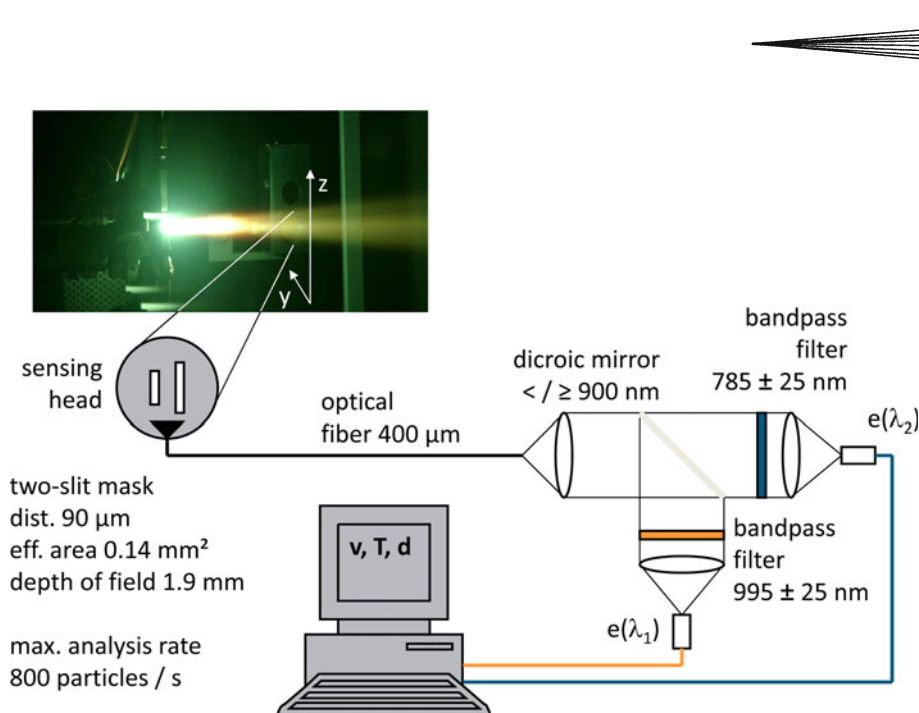


Fig. 7 Measurement setup for the particle diagnostic system DPV-2000

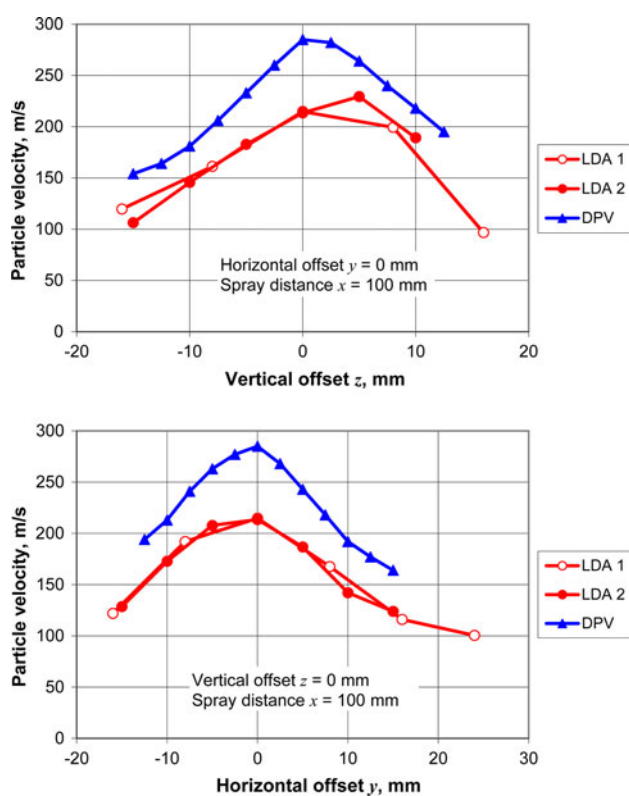


Fig. 8 Vertical and horizontal courses of the LDA and DPV-2000 particle speeds through the measurement grid center points for powder F

that for a given material, there is also a minimum detectable particle size, which is additionally dependent on its temperature. Assuming a particle temperature of 2000°C, the manufacturer of the DPV-2000 indicates that

the detectivity based on the minimum measurable energy ranges down to particle diameters of 14 μm for an emissivity of 0.2, and 8 μm if the emissivity is 0.8. At temperatures higher than 2000°C, even smaller particles are captured. Unfortunately, no precise data are available on the emissivity of molten YSZ. The acceleration of the particles in the plasma plume depends on their masses and thus on the particle diameters. Larger particles tend to have a smaller velocity. The quantitative differences between the velocities measured by LDA and DPV-2000 may be caused by the different detectivities of the two methods. Depending on the particle size, unequal fractions may be captured with different mean velocities. This is investigated in the following.

First, the DPV-2000 results were examined in more detail. As explained above, the system must be calibrated for diameter measurements. This was done using the particle size distribution determined by laser diffraction (see Fig. 5). The calibration factor f_{diam} was set in such a way that the mean diameter d_{50} measured with DPV-2000 agreed with the result of the laser diffraction measurement of the powder feedstock. It should be noted that the feedstock was a spray-dried powder, i.e., many particles were hollow. When they are molten in flight, the diameters of the liquid droplets are certainly smaller. However, since we do not know this effect quantitatively, we could not consider it while calibrating the DPV. Furthermore, the laser diffraction measurement delivers volumetrically weighted frequencies, which must also be accounted for. Thus, the DPV-2000 was operated in the volumetric mode during the calibration procedure. The smallest diameters detected by the DPV-2000 were approximately 6 μm . These particles showed an average temperature of 3055°C, which is considerably higher than the overall mean particle temperature of 2905°C. As smaller particles were obviously not detected by the DPV-2000 in the investigated

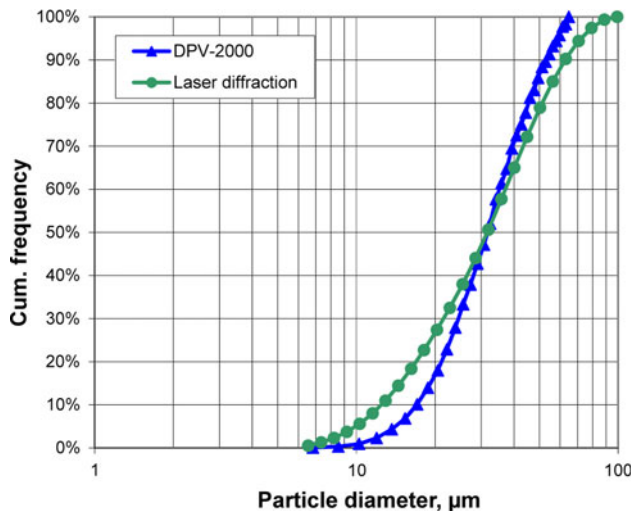


Fig. 9 Volumetrically weighted cumulated frequencies of particle diameters measured by laser diffraction and by DPV-2000 for powder F

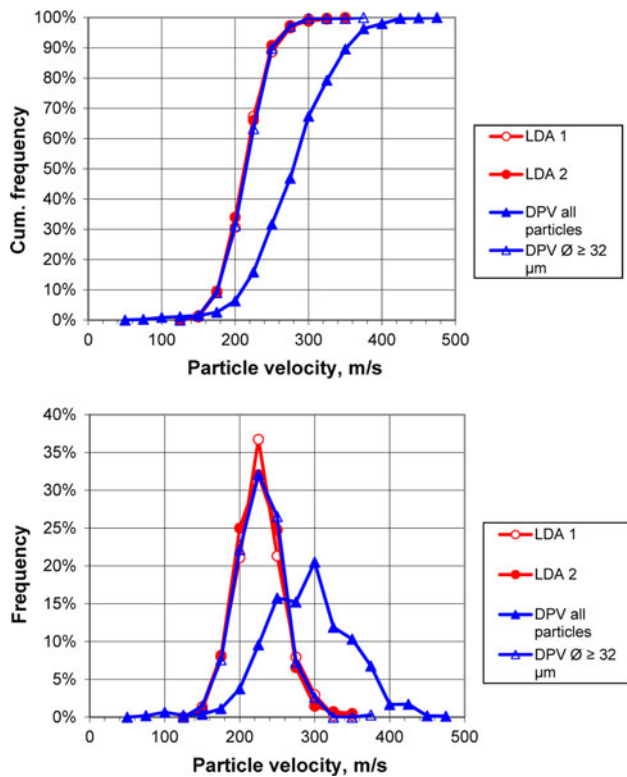


Fig. 10 Comparison of cumulative frequencies (top) and density distributions (bottom) for particle velocities measured using LDA and those obtained by DPV-2000 for powder F

case, particles smaller than $6 \mu\text{m}$ were excluded from the evaluation of the laser diffraction data. This fraction is equivalent to 5.3% of the overall particle volume. Figure 9 shows a comparison of the two cumulated frequency curves. As a result of the DPV-2000 calibration, they intersect at the mean diameter d_{50} . As the curves agree

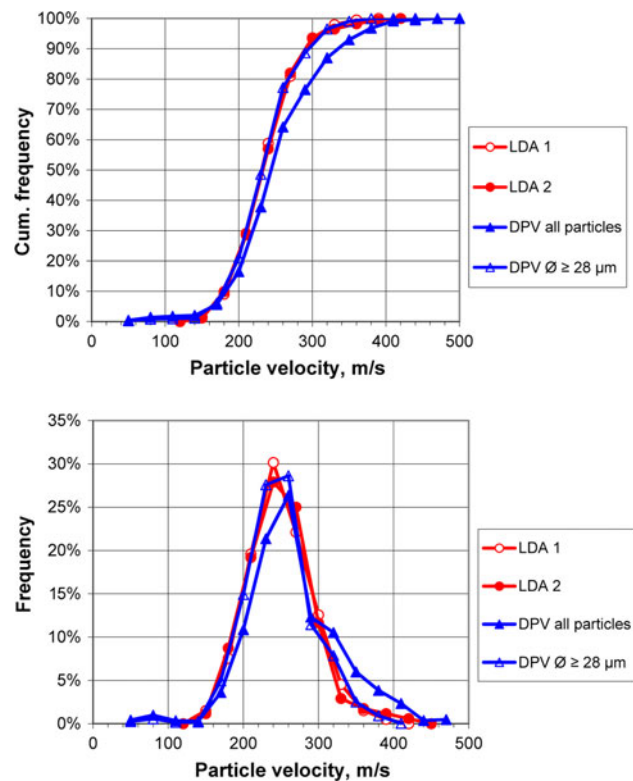


Fig. 11 Comparison of cumulative frequencies (top) and density distributions (bottom) for particle velocities measured using LDA and those obtained by DPV-2000 for powder C

well, it can be concluded that the diameters measured by DPV-2000 are reliable down to a specific detection limit, which was $6 \mu\text{m}$ in this case.

Unfortunately, no quantitative information is available on the detectivity of the applied LDA system. To verify the assumption that a lower detection limit also exists for LDA and that it affects the representativeness of this method, cumulative frequencies and density distributions for the particle velocities of the LDA 1 and LDA 2 measurements as well as for those obtained with DPV-2000 were compared at the center point of the measurement grid. There is a large difference in the mean values between LDA and DPV results, as mentioned above. By evaluating the DPV-2000 results, mean particle velocities were calculated not only for the totality of the detected particles but also for fractions above specific particle diameters. Considering particles with diameters greater or equal to $32 \mu\text{m}$ only, a mean velocity of 214 m s^{-1} was obtained. As smaller and faster particles were excluded, this average velocity was smaller than the mean velocity for the totality of particles. This value corresponds to the LDA results (215 m s^{-1} for LDA 1 measurement and 213 m s^{-1} for LDA 2 measurement). The associated DPV cumulative frequencies and density distribution for this particle fraction are also included in Figure 10. They show very good agreement with the measurement results of LDA 1 and LDA 2. Thus, presuming that no systematic errors occurred, it can be concluded that in the investigated

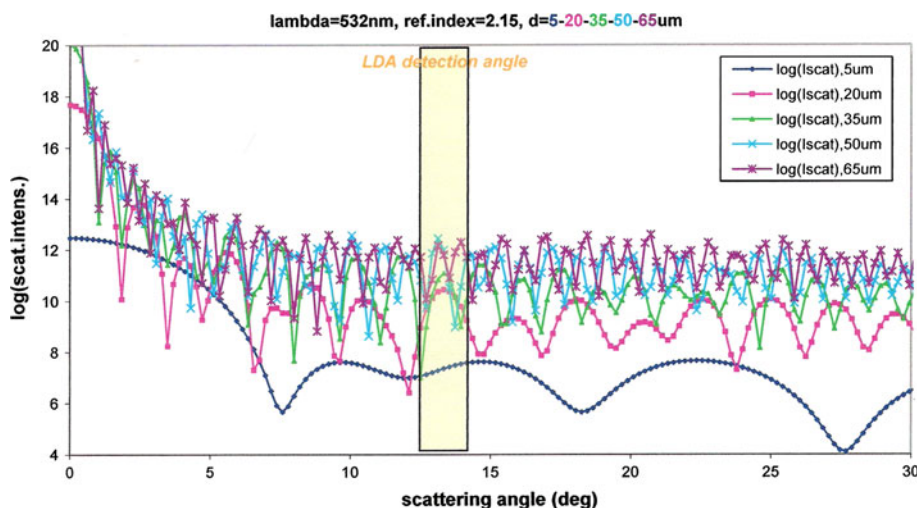


Fig. 12 Scattered intensity of a single spherical particle with diameter d for an incident wavelength of 532 nm and a refractive index of 2.15 (YSZ, no absorption)

case, the lower detectivity limit of the LDA was reached at a particle diameter of 32 μm .

To confirm the assumption of a lower detection limit in LDA, a second set of two LDA measurements and one DPV measurement was performed with the coarser powder C. As before, DPV diameter measurements were calibrated based on the particle size distribution determined by laser diffraction. Figure 11 compares LDA and DPV results. As expected for this coarser powder, the curves are closer to each other because a smaller fraction of the powder particles was subjected to the detection limit of LDA compared with the finer powder F. The best agreement was found when only particles with a diameter $\geq 28 \mu\text{m}$ were considered in the DPV evaluation. This value is quite close to the threshold of 32 μm , which was found for the finer powder F.

A lower detectability threshold for particle diameters of 28–32 μm in LDA is therefore consistent with the intensity scattered by the particles (and detected by LDA). The intensity of the signal depends on the detection angular direction and the object size (particle diameter). Assuming spherical particles and using Mie theory (Ref 21), this angular function can be determined. Figure 12 shows the calculation results for the Mie scattering of nonpolarized light with a wavelength of 532 nm at a single spherical particle of diameter d , carried out using the code developed in Ref 26 and 27. It is obvious that the scattered intensities at YSZ particles with diameters less than 35 μm are at least two orders of magnitude lower than for larger particles. Thus, the conclusion that LDA has a lower detection limit is justified.

5. Conclusion

A lower detectability threshold for particle diameters of 28–32 μm in LDA was found in comparative measurements versus the DPV-2000 diagnostic system. The calculation of the Mie-scattering confirms that this lower

bound for LDA particle size measurement is consistent with the scattered intensities (and detected by LDA). At values greater than this threshold, the results obtained by LDA and DPV particle diagnostic systems are in very good agreement. This is of particular importance, since it could be suggested that the LDA technique for plasma spraying is generally limited by the experimental environment (e.g., plasma fluctuations, huge temperature, and flow velocity gradients).

References

1. L. Pawlowsky, *The Science and Engineering of Thermal Spray Coatings*, John Wiley & Sons, Chichester, UK, 1996
2. P. Fauchais and M. Vardelle, Plasma Spraying: Present and Future, *Pure Appl. Chem.*, 1994, **66**(6), p 1247-1258
3. P. Fauchais, A. Vardelle, and B. Dussoubs, Quo Vadis Thermal Spraying?, *J. Therm. Spray Technol.*, 2001, **10**, p 44-66
4. K. Landes, Plasma Generators for Thermal Plasma Processes, *Int. J. Mater. Res.*, 2011, **102**(8), p 959-963
5. J.-L. Marqués, G. Forster, and J. Schein, Multi-Electrode Plasma Torches: Motivation for Development and Current State-of-the-Art, *Open Plasma Phys. J.*, 2009, **2**, p 89-98
6. G. Gouesbet, A Review on Measurements of Particle Velocities and Diameters by Laser Techniques, with Emphasis on Thermal Plasmas, *Plasma Chem. Plasma Process.*, 1985, **5**(2), p 91-117
7. P. Fauchais, J.F. Coudert, and M. Vardelle, Diagnostics in Thermal Plasma Processing, *Plasma Diagnostics*, O. Auciello and D.L. Flamm, Ed., Academic Press, New York, 1989, p 410-432
8. S. Zimmermann, J. Marques-Lopez, S. Lange, S. Kirner, K. Landes, and J. Schein, Designing, Setting-Up and Application of Mobile Process Diagnostic Systems in the TS Cluster for the Thermal Coating Process, *Therm. Spray Bull.*, 2011, **4**(2), p 148-158
9. M. Hugenschmidt, *Lasermesstechnik, Diagnostik der Kurzzeitphysik* [Laser Measuring, Diagnostics of Short-Time Physics], Springer, 2007, p 131-142
10. F. Mayinger and O. Feldmann, *Optical Measurements-Techniques and Applications*, 2nd ed., Springer-Verlag, Berlin, 2001
11. Tecnar Automation, DPV2000, <http://www.tecnar-automation.com/d/publ-f-e.html>
12. <http://www.dantecdynamics.com/>
13. <http://www.tsi.com/en-1033/index.aspx>

14. <http://www.lavision.de/>
15. <http://www.cyber-materials.com/plasmaspray.html>
16. GALA e.V., Deutsche Gesellschaft für Laser-Anemometrie, <http://www.gala-ev.de/>
17. F. Durst, A. Melling, and J.H. Whitelaw, *Principles and Practices of Laser-Doppler Anemometry*, Academic Press, London, 1976, p 412
18. F. Durst, A. Melling, and J. Whitelaw, *Theorie und Praxis der Laser-Doppler-Anemometrie [Theory and Practice of Laser Doppler Anemometry]*, G. Braun-Verlag, Karlsruhe, 1987
19. H.-E. Albrecht, M. Borys, N. Damaschke, and C. Tropea, *Laser Doppler and Phase Doppler Measurement Techniques*, Springer-Verlag, Berlin, 2003
20. C.S. Johnson, Jr., and D.A. Gabriel, *Laser Light Scattering*, Dover Publications Inc., New York, 1994
21. G. Mie, Beiträge zur Optik trüber Medien, speziell kolloidaler Metallösungen [Contributions on the Optics of Cloudy Media, in Particular of Colloidal Metal Solutions], *Ann. Phys., Fourth series*, 1908, **25**, 330(3), p 377-445
22. G. Mauer, R. Vaßen, and D. Stöver, Comparison and Applications of DPV-2000 and Accuraspray-g3 Diagnostic Systems, *J. Therm. Spray Tech.*, 2007, **16**(3), p 414-424
23. C. Moreau, P. Gougeon, M. Lamontagne, V. Lacasse, G. Vaudreuil, and P. Cielo, On-Line Control of the Plasma Spraying Process by Monitoring the Temperature, Velocity, and Trajectory of In-Flight Particles, *Thermal Spray Industrial Applications*, C.C. Berndt and S. Sampath, Ed., June 20-24, 1994 (Boston, MA), ASM International, 1994, p 431-437
24. G. Mauer, R. Vaßen, and D. Stöver, Detection of Melting Temperatures and Sources of Errors Using Two-Color Pyrometry During In-Flight Measurements of Atmospheric Plasma-Sprayed Particles, *Int. J. Thermophys.*, 2008, **29**, p 764-786
25. S. Zimmermann, E. Vogli, M. Kauffeldt, M. Abdulgader, B. Krebs, B. Rütter, K. Landes, J. Schein, and W. Tillmann, Supervision and Measuring of Particle Parameters During the Wire-Arc Spraying Process with the Diagnostic Systems Accuraspray-g3 and LDA (Laser-Doppler-Anemometry), *J. Therm. Spray Technol.*, 2009, **19**(4), p 745-755
26. C.F. Bohren and D. Huffmann, *Absorption and Scattering of Light by Small Particles*, Wiley & Sons, New York, 1983
27. S. Hanson, Broadening of the Measured Frequency Spectrum in a Differential Laser Anemometer due to Interference Plane Gradients, *J. Phys. D Appl. Phys.*, 1973, **2**, p 164-172